2017 International Symposium on Nonlinear Theory and Its Applications,
NOLTA2017, Cancun, Mexico, December 4-7, 2017

Coupled Piezoelectric Actuators for the Tactile Display

Suketu Naik† and Dhanya Nair†

†Department of Engineering, Weber State University,
1447 Edvalson St. Dept. 1803 Ogden, UT 84408, United States
Email: suketunaik@weber.edu, dhanyanair@weber.edu

Abstract– In this paper, we present an initial study towards using coupled piezoelectric actuators in a tactile display. The focus is on understanding the behavior of a single actuator and its coupled behavior in a grid of actuators. We describe the model of the single actuator using Finite Element Analysis (FEA) and numerical simulations. Next, we apply the model parameters to construct a small grid of actuators and explore the possibility of pattern formation for the haptic feedback.

1. Introduction

Human-Computer Interaction is a novel field with rich applications including virtual reality, haptic feedback, tactile sensation reproduction, and others to provide information on vibration, temperature, shape, texture, etc., to complete the sensors-brain-action loop [1]. One of the main application of a tactile display is to provide assistive technology for the visually impaired. Per World Health Organization, there are 285 million visually impaired people worldwide, and 90% of them live in low-income setting [2]. The cost of commercially available braille displays/assistive tactile devices ranges from $3500 to $15000 depending on the number of Braille cells [3]. Our research aims to study the Braille representation/haptic feedback on a single cell in order to reduce the overall cost of the system. One application is to aid the blind for navigating icons and information displayed by the smart phones and tablets. The challenges for such a device include compactness, power consumption, and an accurate reproduction of the visual information into tactile sensation.

1.1. Haptic Feedback/Tactile Display

At present, there are three major technologies used in the tactile display devices [1]: (1) Devices that control the roughness of the active surface [4][5], (2) Devices that emulate the shape of the visual information using an array of pins [6][7], and (3) Vibro-tactile devices that provide vibrations to the skin using an array of actuators [8]. The devices and system that we are investigating fall between type (2) and (3) above. Our plan is to utilize a 6x6 array of piezoelectric actuators (e.g. fixed-free beams, or fixed-fixed disks) with a small form factor (e.g. 5x5 cm^2) to create an effective tactile display. The choice for the piezoelectric actuators is simple: they provide large deflections through the coupling without introducing complex assembly of parts, at low frequencies involved in tactile sensations (<300 Hz). An additional advantage of the piezoelectric devices is that they can be controlled to create non-contact tactile sensation using ultrasonic vibrations at higher frequencies (~40 kHz) while reducing the grid size. To this end, acoustic multi-touch sensing using wave-diffraction patterns, impact localization techniques for haptic interaction, condensation of ultrasound waves at a focal point, acoustic radiation force, stationary ultrasonic waves to create spatially located haptic image have been explored in [9], [10], [11], [12], [13] respectively.

The goals of this research are to generate: 1) On/Off binary patterns, 2) Sinusoidal wave patterns, and 3) Horizontal and vertical bar patterns; with the overall goal of understanding on how best to present texture and Braille on mobile tactile displays. Goal 1 may be accomplished by actuating individual piezoelectric or inductive devices with very high DC bias such that they act as on-and-off switches. In this paper, we focus on the possibility of addressing the goals 2 and 3 above. In [5], the researchers evaluated the human tactile resolution in terms of signal wavelength and pattern depth on variable friction tactile displays, by utilizing sinusoidal input for texture rendering. [14] demonstrates the presentation of Braille dots through progressive lateral deformation of skin. They utilized a moving wave pattern to create an illusion of a dot moving below the finger. The actuators used in the study had a large form factor restricting the reproduction of entire Braille characters using the same. Coupled actuators using slow moving sinusoidal input could produce the same effect without the aforementioned size constraint. This paper evaluates the coupled piezoelectric actuators based tactile display system when operating with sinusoidal input.

The synchronization phenomena have been explored in depth by several groups and it is well-known that an ensemble of nonlinear elements (e.g. devices, transducers, resonators, oscillators) can be coupled electronically and/or mechanically to generate complex spatio-temporal patterns [15-19]. For sensing, the weakly nonlinear coupled systems offer very high sensitivity and large output signal in the presence of noise due to the synchronized state that tends to be robust to small perturbations. For actuation, the coupled systems have not been studied thoroughly from engineering perspective in either the weakly nonlinear and strongly nonlinear regimes. Here our study is focused on the weakly nonlinear coupled actuators for the purposes of pattern formation.

2. Model of Single Piezoelectric Actuator

There are two primary causes of nonlinearity in a piezoelectric actuator: depolarization of the ferroelectric domains and creep. Depolarization is described by the fact that when a piezo actuator is driven by a strong electric field, its a priori polarization changes and some of ferroelectric domains reorient themselves, which leads to nonlinear behavior. This behavior is exemplified by the hysteresis present in the actuator's polarization vs. electric field curve [20]. Creep is a phenomenon that is immediately followed by depolarization, where the switch in stress (or strain) leads to ringing in time-domain. Creep effect is transient (~100 s) and is usually not included to model the nonlinear behavior [20][21]. While the hysteresis can be described by various models such as Preisach model, Prandtl-Ishlinskii model, or Maxwell Slip model, the nonlinear behavior in general can be attributed to large deformation of the piezo material [21]. To this end, spring-softening has been empirically observed in bimorph fixed-free PZT-5H actuators [22]. Our candidate device is a bimorph fixed-free actuator with PZT-5A material with similar electrical and mechanical properties. We adopt spring-softening to describe the nonlinearity in PZT-5A since we lack the experimental data on our actuator at the moment.

2.1. FEA Simulations

The actuator layers are as follows: Kapton with Cu electrodes as top, middle, and bottom (1.5 mil each) layers, two PZT-5A as the piezoelectric layers (8 mil each) in the middle. The thicknesses of the layers and distributions of the two bimorph actuators were simplified to form a single actuator as shown in Fig. 01a. The above actuator and its fundamental eigen-mode are depicted in Fig. 01b. The first three eigen-modes were observed at 133.13 Hz, 661.03 Hz, and 1258.3 Hz in the FEA (Comsol) simulation. Fig. 02a depicts the frequency response of the displacement amplitude in z-dir while applying a sinusoid voltage with $100V_{amp}$ between the top and bottom electrodes (100 V is the drive limit for the Mide Shivr SP-21B beam) and by varying its frequency. This simulation does not include nonlinear effect. The resonance frequency was verified as ~133 Hz. This was verified in the time-domain with excitation voltage = $100V_{amp}$.

2.2. Numerical Simulations

Single actuator beam can be described in dimensionless form as,

$$z'' + \delta z' + z + \beta z^3 = \varepsilon \cos \omega\tau - \varepsilon_o \quad \text{........ (1)}$$

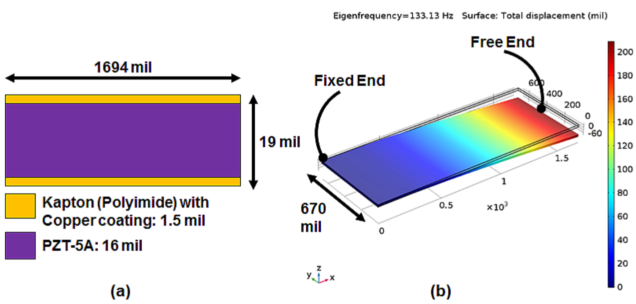

Fig. 01: FEA simulations: (a) Simplified layers of Mide Shivr SP-21B bimorph actuator, (b) Fundamental eigen-mode at 133.13 Hz.

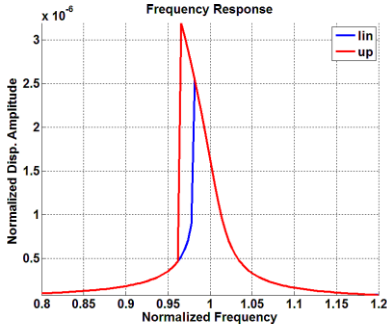

Fig. 02: Numerical simulations: soft-spring effect based on (1) using 4th order Runge-Kutta method. Note that ε_o=0.

where, z=tip displacement in z-direction with $'$ and $''$ as the 1st and 2nd second order derivatives w.r.t. normalized time τ, δ=normalized damping=$c/m\omega_o$, β=normalized nonlinear spring constant=k_3/k_1, ε=normalized piezoelectric force amplitude=nV_a/k_1, ε_o=normalized finger-tip force=F_{ext}/k_1, where m=mass [kg], c=damping [Ns/m], $\omega_o=2\pi f_o$=resonance frequency [rad/s], k_3 = cubic spring constant [kg/m^3], k_1=linear spring constant, n=electromechanical coupling constant [N/V], V_a=amplitude of the driving voltage [V], F_{ext}=fingertip force [N], ω_d=driving frequency [rad/s], and $\tau = \omega_o t$. The above parameters were derived from the beam geometry, FEA simulations shown in Fig. 01, and literature with similar beam structures [20-22]. Fig. 02 shows the soft-spring effect after simulating (1) as a system of 1st order equations with $\beta<0$ to assert the bistable potential function. Here, we assume that ε_o=0 because the DC force pre-loads the actuator and it is constant throughout the operation as it emulates a person resting his/her finger on the actuator tip in the tactile display. Moreover, the pre-loading force itself may contribute to the bistable potential in the actuator as noted in [22].

3. Coupled Piezo Actuators

In this section, we model and simulate the dynamics of the coupled system of piezo actuators. First, we present a 1-D (in the x-dir) coupled system of actuators as a chain. We formulate the problem of the coupled system of actuators as activator-inhibitor system (reaction-diffusion type) by applying the piezo force to the left-most actuator. We analyze the synchronization from the perspective of the phase dynamics. Here our goal is to answer the following question: which of the following factors are useful for the pattern control: initial conditions, boundary conditions, inhomogeneities, or symmetry-breaking? For the sake of simplicity, we assume that the 6x6 grid of Piezo actuators, as shown in Fig. 03, will consist of six individual 1-D chains. Here, the chains are excited uniformly with an applied voltage on one end. The other ends of the chains are grounded thus representing the terminations. This implementation will not allow back propagation of the coupled waveforms from the grounded ends and therefore the dependence on boundary conditions can be omitted. The initial conditions of the piezo actuators will be

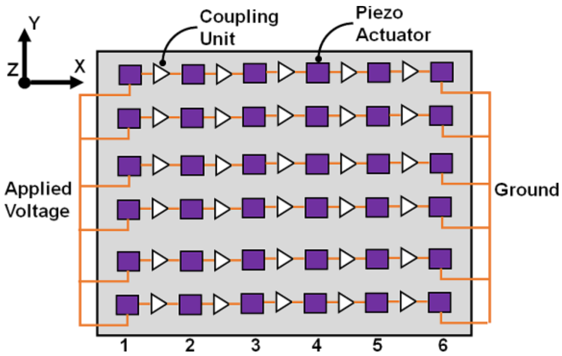

Fig. 03: Proposed system of coupled actuators: Here, the entire 6x6 grid consists of six 1-D chains with an identical applied voltage and ground. Coupling unit=amplifier or resistor.

assumed as $z = z' = 0$. The coupled system will be homogenous since the coupling function is identical for each set of actuators. Now, the only remaining factor is *symmetry-breaking* in the coupled system of actuators. Moreover, the parameter space is quite large with ε and λ as the attractive parameters, which create phase synchrony, and ω , which creates the detuning or repulsive behavior.

3.1 Coupling

Global coupling through driving force or nearest neighbor coupling between two oscillators plays a key role in that it allows the phase dynamics of the coupled ensemble to transition from equilibrium points to periodic, quasiperiodic, chaotic, and hyperchaotic behaviors [23]. Here, our goal is to analyze *symmetry breaking* behavior of the coupled ensemble through a certain coupling scheme that can generate stable periodic solutions so that they can be turned spatially and temporarily. To this end, we build our behavioral model based on diffusive coupling scheme while considering a unidirectional system (an inductor can induce bidirectional coupling but we omit it due to a risk of short-circuiting).

3.1.1 Diffusive Coupling

This type of coupling happens when two resonators are connected via resistors [24]. In a chain of actuators, this is only possible if the piezoelectric actuators allow three separate contact pads: one for excitation signal (driving signal or coupling signal), one for sensing, and one for ground. The coupled system of 1-D chain with diffusive coupling can be represented by the following equation:

$$z_1'' + \delta z_1' + z_1 + \beta z_1^3 = \varepsilon \cos \omega\tau$$
$$z_m'' + \delta z_m' + z_m + \beta z_m^3 = \lambda(z_{m-1} - z_m)$$

where m=2…6 ……………………………………. (2)

Here, λ= coupling strength set by a resistor. The stability of the synchronous equilibrium was verified by plotting Asymptotic Continuous Spectrum(ACS) curves for each actuator [23]. As shown in Fig. 04, the equilibrium becomes unstable past the critical value of λ as indicated by

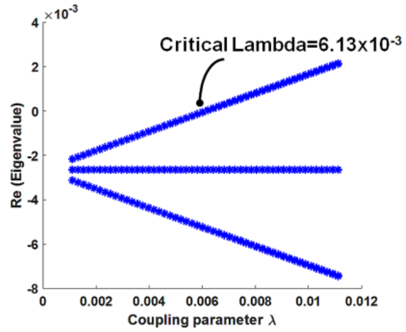

Fig. 04: Stability of equilibrium: the real part of eigenvalue becomes positive past the critical value=6.13x10^{-3} indicating instability of the equilibrium point $z = z' = 0$.

the real part of the eigenvalues becoming positive. For the 1-D chain of actuators, this value indicates the point at which the amplitude of the oscillations grows rapidly and the oscillations show phase-synchronization with each other as the λ is swept from left to right. Immediately past this value, the current system shows three distinct phase-synchronization states between two neighboring elements for specific values of the excitation amplitude ε at a fixed **ω=1** (no detuning) as shown in Fig. 05: 1) 2π/6 phase difference, 2) 2π/3 phase difference with adjacent neighbors and 0 phase difference with its symmetric elements (e.g. P1-P4, P2-P5, P3-P6), and 3) random or varying phase difference.

The stability of the periodic solutions was verified by analyzing the Floquet multipliers (eigenvalues of the mondromy matrix) of the linearized Pointcare map. Here, one complex conjugate pair stays on the unit-circle per the Floquet theory [25]. The other complex conjugate pairs stay within the unit circle for case (a) and (b) in Fig. 05 indicating stable solutions. For case (c), one pair seems to

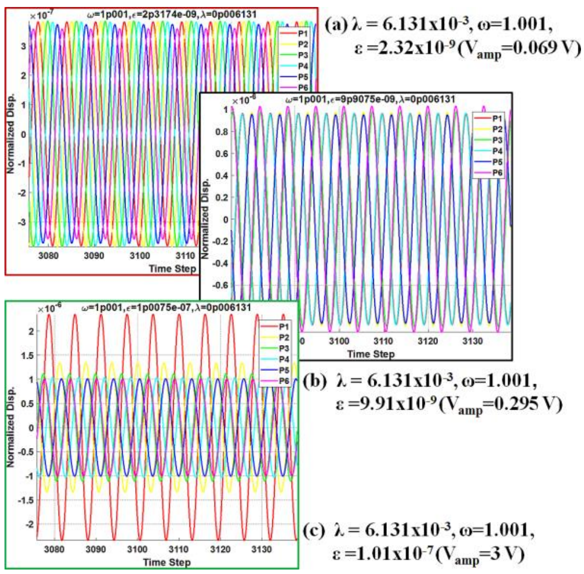

Fig. 05: Periodic solutions with ω=1, λ=6.131x10^{-3} while varying ε in (2): (a) 2π/6 phase difference, (b) 2π/3 phase difference between pairs P1-P4, P2-P5, P3-P6, and (c) desynchronized state.

exit the unit circle on the imaginary axis indicating unstable or marginally stable solutions.

Additionally, the simulations in the parameter space (***ε, λ, ω***) show the following: (a) the coupled system remains stable and synchronized within wide range of the coupling strength while varying ***ε*** at ***ω*=1** (b) the coupled system remains stable and synchronized within a narrow range of the detuning parameter ***ω*** while varying ***λ*** at a small ***ε***.

4.0 Future Work

Current study shows that distinct types of oscillations can be created and controlled for both the contact-based or non-contact tactile display that we will explore in future. The future work in this project includes detailed simulation and experimental analyses of 2-D (*x,y*) coupled system in which the coupling can be realized either as an amplifier or a resistor. The case of resistive coupling offers a simpler solution and will make the implementation easier.

Acknowledgments

The authors would like to thank the personnel at the Utah School for the Deaf Blind (Ogden, Utah), Dr. Justin Jackson (Weber State University) and Mr. Suny Ly (Weber State University) for insightful discussions and comments.

References

[1] J. Streque, et. al., "New Magnetic Microactuator Design Based PDMS Elastomer and MEMS Technologies for Tactile Display," *IEEE Transaction on Haptics*, vol.3, no. 2, pp.88-97, 2010.

[2] World Health Organization, "Fact sheet," http://www.who.int/mediacentre/factsheets/fs282/en/

[3] American Foundation for the Blind, "Refreshable Braille Displays," http://www.afb.org

[4] S. Chu, et. al., "Experimental Evaluation of Tactile Patterns over Frictional Surface on Mobile Phones," *Proceedings of the Fifth International Symposium of Chinese CHI,* pp. 47-52, 2017.

[5] J. Kim, et. al., "An Empirical Study of Rendering Sinusoidal Textures on an Ultrasonic Variable Friction Haptic Surface," *12th International Conference on Ubiquitous Robots and Ambient Intelligence (URAI),* pp. 593-596, 2015.

[6] M. Tezuka, et. al., "Micro-needle electro-tactile display," *37th Annual International Conference of the IEEE Engineering in Medicine and Biology Society (EMBC)*, pp. 5781-5784, 2015.

[7] S. Khurelbaatar, "Tactile Presentation to the Back of a Smartphone with Simultaneous Screen Operation," *Proceedings of the 2016 CHI Conference Extended Abstracts on Human Factors in Computing Systems*, pp. 281-284, 2016.

[8] R. Hatada, et. al., "Haptoskin - A flexible sheet-type tactile display with a CNT electrode," *29th IEEE International Conference on Micro Electro Mechanical Systems*, 2016, pp. 1145-1148.

[9] Y. Liu, et. al., "An Acoustic Multi-touch Sensing Method using Amplitude Disturbed Ultrasonic Wave Diffraction Patterns," *Sensors and Actuators A: Physical*, vol.162, no. 2, pp.394-399, 2010.

[10] S. Wockel, et. al., "Ultrasonic Time Reversal for Haptic Interaction," *AMA Conferences: Sensors 2015 P3.2*, pp. 769-77, 2015.

[11] M. Ciglar, "An Ultrasound Based Instrument Generating Audible and Tactile Sound," *Proceedings of 2010 Conference on New Interface for Musical Expression*, pp. 19-22, 2010.

[12] B. Long, et. al., "Rendering Volumetric Haptic Shapes in Mid-air using Ultrasound," *ACM transactions on Graphics*, vol. 33, no.6, pp. 181.1-181.10, 2014.

[13] S. Inuoe, et. al., "Active Touch Perception Produced by Airborne Ultrasonic Haptic Hologram," *IEEE World Haptics Conference*, pp. 362-367, 2015.

[14] V. Lévesque, et. al., "Display of Virtual Braille Dots by Lateral Skin Deformation: Feasibility Study," *ACM Transactions on Applied Perception (TAP),* vol. 2, no. 2, pp. 132-149, 2005.

[15] A. Pikovsky, et. al., *Synchronization: A Universal Concept in Nonlinear Sciences*. Cambridge University Press, 2001.

[16] S. Naik, et. al., "Local Bifurcations of Synchronization in Self-excited and Forced Unidirectionally Coupled Micromechanical resonators," *Journal of Sound and Vibration*, vol. 331, no. 5, pp. 1127–1142, 2011.

[17] S. H. Strogatz, *Nonlinear Dynamics and Chaos: With Applications to Physics, Biology, Chemistry, and Engineering*. Reading: Addison-Wesley, 1994.

[18] V. In, et. al. "Frequency down-conversion using cascading arrays of coupled nonlinear oscillators," *Physica D: Nonlinear Phenomena*, vol. 240, no. 8, pp. 701-708, 2011.

[19] B. Meadows, et. al., "Nonlinear Antenna Technology," *Proceedings of the IEEE*, vol. 90, no. 5, 2002.

[20] M. Hudek, *Modeling and control of a piezoelectric actuator for active and adaptive optics*, B.S. Thesis, Czech Technical University, 2013.

[21] H. Richter, et. al., "Modelling Nonlinear Behavior in a Piezoelectric Actuator," *Precision Engineering,* vol. 25, no. 2, pp. 128-137.

[22] R. Wood, et. al., "Nonlinear Performance Limits for High Energy Density Piezoelectric Bending Actuators," *Proceedings of the IEEE International Conference on Robotics and Automation*, 2005.

[23] P. Perlikowski, et. al., "Routes to complex dynamics in a ring of unidirectionally coupled systems," Chaos, 20, 013111, 2010.

[24] H. Kitajima, et. al., "Bifurcation and chaos in unidirectionally," *Proc. NOLTA'97*, pp.65-68,1997.

[25] R. Seydel, *Practical Bifurcation and Stability Analysis*. Springer-Verlag, 1994.

[26] Ando., et. al., "Nonlinear Electric Field Sensor That Exploits Coupled Oscillator Dynamics," *IEEE Transactions on Instrumentation and Measurement*, vol. 62, no.5, 2013.